THE JOURNAL OF PHYSICAL CHEMISTRY B LETTERS

2007, *111,* 3077−3080
Published on Web 03/03/2007

Magnetically Driven Colloidal Microstirrer

Pietro Tierno,*,† Tom H. Johansen,‡ and Thomas M. Fischer†

Department of Chemistry and Biochemistry, Florida State University, Tallahassee, Florida 32306-4390, Department of Physics, University of Oslo, P.O. Box 1048, Blindern, Norway

Received: January 23, 2007; In Final Form: February 15, 2007

Paramagnetic colloidal particles dispersed in water and deposited above magnetic bubble domains of a uniaxial ferrimagnetic garnet film are used as microscopic stirrer when subjected to external rotating magnetic fields. The hydrodynamic flow field above the stirrer is detected by tracking of nonmagnetic microspheres. The vorticity of the flow falls off inversely proportionally to the distance from the bubble center and is proportional to the field frequency. The device provides complete control over the mixing capability. This alternative method of active mixing might be used for microfluidics applications where mechanical stirring cannot be achieved easily with other machinery parts.

1. Introduction

Mixing is an important process in analytical,[1] chemical,[2] and biological[3] research. When applied to microfluidics, mixing of small volumes of fluids is difficult due to the fact that, at low Reynolds number, turbulent flow is suppressed.[4−6] Successful performance of integrated lab-on-a-chip devices depends on how rapid small volumes of reactants are mixed together. When two miscible fluids merge into a common channel, mixing is diffusive and thus can be comparably slow.[7,8] Another approach is to use chaotic advection by driving the reactant through serpentine, twisted, and interconnected structures.[9] In microscopic applications, where both mechanisms are not sufficient to achieve efficient mixing, alternative methods such as active "stirring"[10] need to be used.

Current active mixers, like mechanical stirrers, require external machinery[11] and involve moving parts.[12] The incorporation of those stirrers into the predefined and nonreconfigurable patterns of the peripheral arrangement of the rest of the microfluidic device requires complex combined micromechanical engineering.[13] It has been recently demonstrated by Terray, Oakey, and Marr,[14] that colloidal particles can be used as active flow-control elements in integrated microfluidic devices. The advantage, other than monodispersity and size tunability, is that these particles can be easily manipulated with the aid of relatively small and noninvasive external fields.[15] On the basis of this concept, one can use external magnetic field gradients to move paramagnetic particles in a liquid medium and thus drag or even mix small volumes of reactants.

In this letter, we describe a magnetically driven active mixer based on paramagnetic particles placed on top of ferromagnetic bubble domains that are subjected to rotating magnetic fields. We measure the vorticity of the flow field generated by the rotating particles by tracking the position of small tracer spheres dispersed in water above the mixers. By varying the rotation frequency of the external field, we may adjust the stirring rate of the paramagnetic particles and thus increase (or decrease) the stirring capability of our device.

2. Experimental Section

The magnetic bubble lattice was created by using a ferrite garnet film of composition $Y_{2.5}Bi_{0.5}Fe_{5-q}Ga_qO_{12}$ ($q = 0.5-1$), thickness $\sim 4\ \mu$m and saturation magnetization $M_s = 1.7 \times 10^4$ A/m, which was epitaxially grown on a gadolinium gallium garnet substrate. A series of high-frequency magnetic field pulses normal to the film ($\Omega = 12 \times 10^3\ s^{-1}$, $H_0 = 5.0 \times 10^4$ A/m) enforce the formation of a magnetic bubble domain pattern. The pattern is characterized by a series of cylindrical ferromagnetic domains with diameter $2R = 9.2 \pm 0.1\ \mu$m and magnetization normal to the film, separated by a continuous domain film having opposite magnetization direction.[16] We coated the garnet film with a thin layer of polysodium-4-styrene sulfonate[17] to prevent adhesion of the colloidal particles on the film. As colloidal stirrers, we used polystyrene paramagnetic particles with diameter of $2a = 2.8 \pm 0.1\ \mu$m and effective magnetic susceptibility $\chi = 0.17$ (Dynabeads M-280). The particles were electrostatically stabilized in water at a concentration of $\sim 2 \times 10^9$ beads/mL due to the dissociation of surface carboxylic groups (COO^-). As tracer particles, we used nonmagnetic polystyrene particles of diameter $2a = 0.99 \pm 0.05\ \mu$m and density 1.2 g/cm^3 dispersed in water at $\sim$10% concentration by weight. The original suspension of the paramagnetic particles was diluted with deionized water up to a concentration of $\sim 7 \cdot 10^6$ beads/mL, and a small drop of $\sim$5 mm diameter was gently placed on top of the garnet film. The particles sedimented in water and approached the solid−liquid interface because of gravity (particle density 1.4 g/cm^3) but did not adhere due to the electrostatic repulsion with the polymer coated surface of the garnet film. As a consequence, the particles levitated a few nanometers above the garnet film surface. Here they felt the magnetic stray field of the bubble domain pattern and became pinned to the domain walls.[18]

* Corresponding author. E-mail: ptierno@chem.fsu.edu. Telephone: +1-850-645-7442.
† Department of Chemistry and Biochemistry, Florida State University.
‡ Department of Physics, University of Oslo.

10.1021/jp070579o CCC: $37.00 © 2007 American Chemical Society

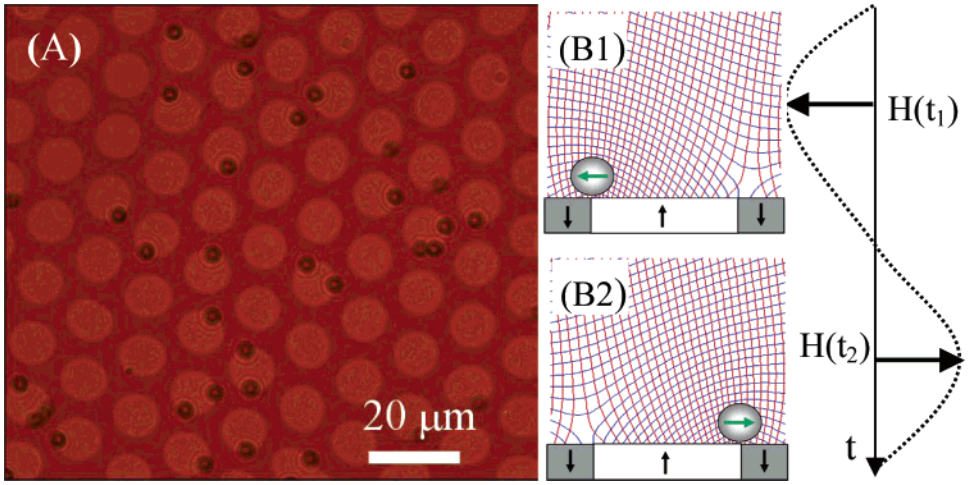

Figure 1. (A) Paramagnetic polystyrene particles floating on top of a ferromagnetic garnet film with a magnetic bubble array. (B1) and (B2) schematic showing the cross-section of a magnetic bubble and the position of the particle at two different times (t_1, and $t_2 = t_1 + \pi/\Omega$). Superimposed on the scheme are the magnetic field lines (blue), the equipotential lines (red), and the induced particle moment (green). The direction of the external magnetic field is shown on the right.

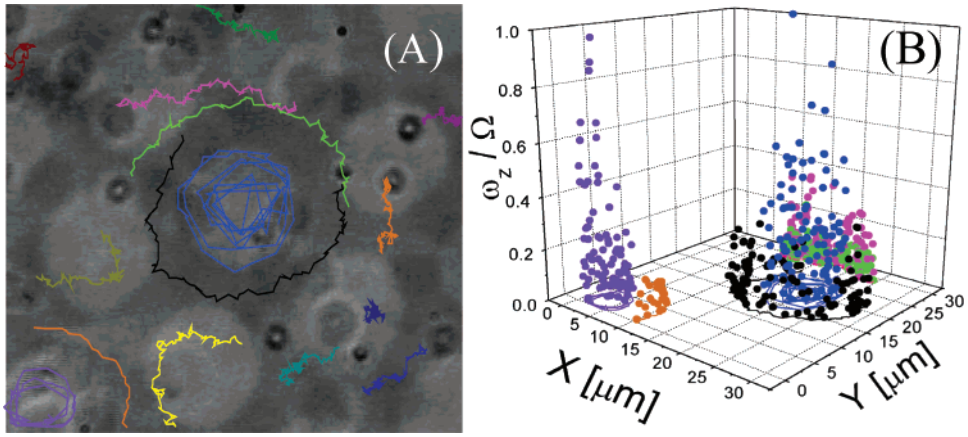

Figure 2. (A) Polarization microscope image showing the tracer colloidal particles ($2a = 1.0$ μm diameter) on top of the bubble lattice with the tracer trajectories superimposed. The paramagnetic stirrers and the garnet film are out of focus because they lie below the focal plane that was adjusted to the tracer particles. (B) 3D plot of the vorticity ω_z normalized with respect to the field frequency Ω. Projected in the *xy* plane are the corresponding particle trajectories. Here, the external magnetic field had an amplitude of $H_0 = 2.06 \times 10^3$ A/m and rotation frequency $\Omega = 94.2$ s^{-1}. A movie of the tracer particle motion can be viewed in the Supporting Information.

To create a stirrer, we mixed the paramagnetic particle water suspension with a stock solution of the tracer spheres (1:10 ratio by weight) and deposited the resulting suspension on the garnet film. Then, a rotating in-plane magnetic field was applied using two orthogonal pairs of coils. The particles were imaged with a Leica DMPL polarization microscope used in transmission mode (the magnetic film is transparent under visible light). Polarization microscopy was used to simultaneously visualize the magnetic bubble domain pattern in the film via the polar Faraday effect,[19] which lets the continuous downward magnetized domain appear darker than the upward magnetized bubble domains (Figure 1A). Videos for image analysis were taken with a color CCD camera (Basler, A311F) at 30 fps (Figure 1A) or with a b/w fast camera (Fastcam Super 10 K, Photron) at 125 fps (Figure 2A).

3. Results and Discussion

Shown in Figure 1A is a polarization microscopy image of a garnet film with magnetic bubble domains having an aqueous solution of paramagnetic particles deposited on top of the film. The general principle used to rotate the particles is schematically depicted in Figure 1, B1−B2. The schematics (B1) and (B2) show the cross-section of a magnetic bubble and the position of the paramagnetic particles at two times, t_1 for B1 and t_2 for B2, separated by half the period of the in-plane magnetic field rotation. When subject to an external magnetic field, the particles of volume V and effective magnetic susceptibility χ acquire a magnetic moment $\vec{m} = \chi V \vec{H}$ that points along the magnetic field direction. The magnetic landscape generated from the garnet surface and the external field thus affects the particles positions on the bubble. The external magnetic field rotates in-plane with a frequency Ω and amplitude H_0, $\vec{H}_{ext} = H_0(\sin \Omega t, \cos \Omega t, 0)$ and modifies the magnetic field distribution *above* the garnet film. Because of its small strength, $H_0 < 1 \times 10^4$ A/m, the in-plane magnetic field does not modify the magnetic bubble domain pattern. Because the magnetic field is quasistatic, we may write it as the gradient of a scalar magnetostatic potential $\mathbf{H} = \nabla\psi$. We calculate the magnetic field lines (blue) and the equipotential line (red) and superimpose them to the images. The green arrows on the magnetic beads indicate the induced magnetic moments of the particles. Here we approximate the paramagnetic particles as point particles placed above the film at an elevation that equals the radius of the spheres. The particles move with the rotating field by describing a circle with a radius equal to the bubble radius R. The particles were found to synchronously follow the field dynamics up to angular frequency

of $\Omega \sim 250\ s^{-1}$. For higher frequencies $\Omega > 250\ s^{-1}$, asynchronous motion eventually occurs presumably due to hydrodynamic friction between the sphere and the polymer surface of the garnet film.

The rotating spheres in a viscous liquid generate a vortical flow field that can be used to move or mix different liquids. We quantify the stirring capability of the rotating particles in water by placing small nonmagnetic spheres floating above the stirrers. Using videomicroscopy and consecutive particle tracking, we determine the position and the motion of several tracer spheres in a common focal plane (approximately 5 μm above the surface of the film). Figure 2A shows a microscope image of the nonmagnetic particles with their trajectory when the system has been subjected to an external magnetic field having amplitude $H_0 = 2 \times 10^3$ A/m and rotation frequency $\Omega = 94.2\ s^{-1}$. The tracer spheres, deposited above the stirrers, acquire an azimuthal velocity that depends on the distance of the tracer particle to the closest bubble domain center. We measure the z component of the vorticity ω_z by measuring the in-plane component of the fluid velocity (v_y,v_x) and then numerically compute the normal component of the vorticity:

$$\omega_z = \partial_x v_y - \partial_y v_x \quad (1)$$

In Figure 2B, we plot ω_z as a function of the particle position in a 3D graph (projected on the (x,y) plane are the particle trajectories). The vorticity has a maximum value of $\omega_z \sim 0.9\ \Omega$ above the bubble domain center and then decreases to $\omega_z \sim 0.2\ \Omega$ at a distance of $r \sim 7\ \mu$m from the bubble center. Note that the graph shows two paramagnetic stirrers separated by a center to center distance of 24.1 μm. The kinetics of the tracer colloidal spheres located above the stirrers is quite similar for both vortices. No vorticity was detected at a distance larger than $r = 8\ \mu$m from the center of the vortices. However, the extension of the hydrodynamic vortex can be easily and precisely tuned by increasing/decreasing the frequency of the external field.

We analyzed the motion of the tracer particles when transported by the circular vortices generated by the rotating particles. In a stationary and creeping flow approximation, the governing equation for the fluid flow vorticity, $\omega = \nabla \times \mathbf{v}$ takes the form of a Laplace equation, $\nabla^2\omega = 0$. As a consequence, the simplest solution predicts behavior according to:

$$\omega_z \propto 1/r \quad (2)$$

Figure 3 shows the average value of the normal component of the vorticity normalized with respect to the field frequency as a function of the radial distance from the bubble center for different frequencies of the external field. For all the Ω values, the central flow decays with the radial distance and becomes negligible at distances larger than $\sim$13 μm. We used eq 2 to fit the vorticity values and obtain a reasonable agreement with the experimental data (continuous line Figure 3).

The direction of the flow field can be easily reversed by changing the magnetic field polarity. The experiments were performed with 1 μm sized colloids, and the stirring capability is limited by the Brownian motion of these particles. Larger particles (radius > 5 μm) show less thermal motion but tend to sediment. By tracking one individual colloidal sphere located at a large distance from the center of the stirrers, we measured a particle diffusion coefficient close to the theoretical value predicted for a freely diffusing sphere in a fluid bulk,[20] indicating that hydrodynamic interaction with the garnet surface is negligible. The vorticity flow generated also depends on the size of the particles used. Smaller paramagnetic particles reduce the amount of fluid dragged along the particle during rotation and thus decreases the stirring. Larger particles experience larger friction from the surface. They require larger magnetic bubbles to support effective stirring and rely on the use of a different garnet film. Occasionally, we observed that more than one paramagnetic particle is trapped in the magnetic bubble (see Figure 1). Our measurements only account for those events were there is one single colloidal particle at the magnetic bubble interface.

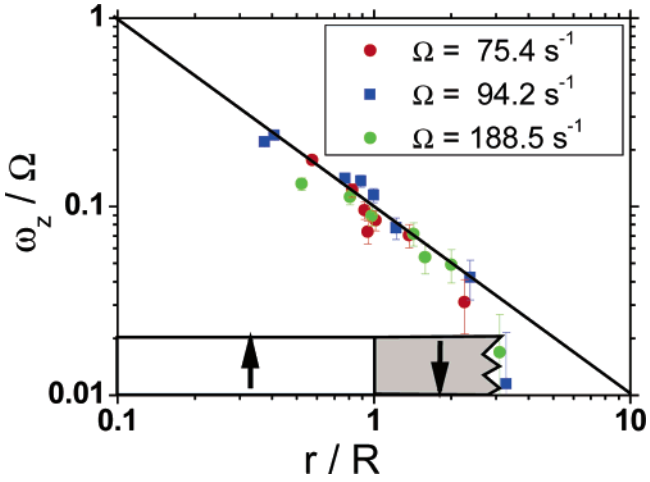

Figure 3. Double logarithmic plot of the normalized vorticity ω_z as a function of the radial distance measured in terms of the bubble radius R. The continuous line is a theoretical fit of the experimental data points according to eq 2.

4. Conclusions

We showed that a magnetic bubble domain pattern provides a novel approach for active stirring of a fluid that may be used for microfluidic devices. The method allows precise tuning of the speed of the rotating particle up to angular frequencies of $\Omega \sim 250\ s^{-1}$ by applying relatively small magnetic fields. We find that the behavior of the generated hydrodynamic vortical flow can be described by a vorticity field inversely proportional to the radial distance from the bubble center. Our stirrer's rotation is limited by the size of the magnetic bubble domains; however, realization of different garnet films with larger or smaller bubble domains and/or use of different size paramagnetic particles would allow further tuning of the mixing capability in integrated lab-on-a-chip devices.

Supporting Information Available: Movie of the microstirrer in action and movie of the tracer particle motion above the microstirrer (MPEG). This material is available free of charge via the Internet at http://pubs.acs.org.

References and Notes

(1) Pamme, N. *Lab Chip* **2006**, *6*, 24.
(2) Becker, H.; Locascio, L. E. *Talanta* **2002**, *56*, 267.
(3) Burns, M. A.; Johnson, B. N.; Brahmasandra, S. N.; Handique, K.; Webster, J. R.; Krishnan, M.; Sammarco, T. S.; Man, P. M.; Jones, D.; Heldsinger, D.; Mastrangelo, C. H.; Burke, D. T. *Science* **1998**, *282*, 484.
(4) Stremler, M. A.; Haselton, F. R.; Aref, H. *Philos. Trans. R. Soc. London, Ser. A* **2004**, *362*, 1019.
(5) Tabeling, P.; Chabert, M.; Dodge, A.; Jullien, C.; Okkels, F. *Philos. Trans. R. Soc. London, Ser. A* **2004**, *362*, 987.
(6) Stone, H. A.; Stroock, A. D.; Ajdari, A. *Annu. Rev. Fluid Mech.* **2004**, *36*, 381.
(7) Branebjerg, J.; Gravesen, P.; Krog, J. P.; Nielsen, C. R. *Proc. IEEE Micro Electro. Mech. Syst.* **1996**, 441.
(8) Schwesinger, N.; Frank, T.; Wurmus, H. *J. Micromech. Microeng.* **1996**, *6*, 99.

(9) Stroock, A. D.; Dertinger, S. K. W.; Ajdari, A.; Mezic, I.; Stone, H. A.; Whitesides, G. M. *Science* **2002**, *295*, 647.
(10) Lu, L.-H.; Ryu, K. S.; Liu, C. *J. Micromech. Syst.* **2002**, *11*, 462.
(11) Okkels, F.; Tabling, P. *Phys. Rev. Lett.* **2004**, *92*, 038301.
(12) Studer, V.; Hang, G.; Pandolfi, A.; Ortiz, M.; Anderson, W. F.; Quake, S. R. *J. Appl. Phys.* **2004**, *95*, 393.
(13) Squires, T. M.; Quake, S. R. *Rev. Mod. Phys.* **2005**, *77*, 977.
(14) Terray, A.; Oakey, J.; Marr, D. W. M. *Science* **2002**, *296*, 1841.
(15) Biswall, S.; Gast, A. P. *Anal. Chem.* **2004**, *76*, 6448.
(16) Babcock, K. L.; Westervelt, R. M. *Phys. Rev. A* **1989**, *40*, 2022.
(17) Helseth, L. E.; Wen, H. Z.; Fischer, T. M.; Johansen, T. H. *Phys. Rev. E* **2003**, *68*, 011402.
(18) Helseth, L. E.; Wen, H. Z.; Hansen, R. W.; Johansen, T. H.; Heinig, P.; Fischer, T. M. *Langmuir* **2004**, *20*, 7323.
(19) *Magneto-Optical Imaging*; Johansen, T. H., and D. V. Shantsev, D. V., Eds.; NATO Science Series II: Mathematics, Physics and Chemistry 142; Kluwer Academic Publishers: Dordrecht, The Netherlands, 2004.
(20) Russel, W. B.; Saville, D. A.; Schowalter, W. R. *Colloidal Dispersions*; Cambridge University Press: New York, 1995; p 51.